

PAPER

[View Article Online](#)
[View Journal](#) | [View Issue](#)Cite this: *Dalton Trans.*, 2022, **51**, 18010

Synthesis and spectroscopic identification of nickel and cobalt layered hydroxides and hydroxynitrates†

Samuel P. Wallbridge,^a Kurt Lawson,^a Amy E. Catling,^a Caroline A. Kirk^b and Sandra E. Dann^{*a}

The formation of different nickel and cobalt layered hydroxide phases by a variety of solution and solid-state synthesis methods has been investigated. Initially, preparative methods were refined to generate single-phase products from metal(II) nitrate hexahydrate starting materials which were then characterised by powder X-ray diffraction, vibrational spectroscopy and thermogravimetric analysis. As well as the brucite type β -M(OH)₂ and the hydrotalcite-like [M(OH)_{2-x}(H₂O)_x]^{x+} alpha-phases (where M = Ni, Co), two different hydroxynitrate phases were isolated with the generic formula M(OH)_{2-x}(NO₃)_x with $x = 0.67$ and 1.0 (where M = Ni, Co). The reduction of symmetry of the nitrate anion from D_{3h} to C_{2v} allows the alpha-phases to be distinguished from the two different layered hydroxynitrate phases by both infrared and Raman spectroscopy through the loss of symmetry and concomitant splitting of the degenerate bands. The symmetric N–O stretch enables the two hydroxynitrate phases to be distinguished from one another through the sharp absorption bands at *ca.* 1000 cm⁻¹ ($x = 0.67$) and *ca.* 1050 cm⁻¹ ($x = 1.0$). The thermogravimetric analysis data of the phases showed key differences between the layered hydroxides, with anhydrous phases having singular weight losses over short temperature ranges and hydrated phases having multiple losses over more extended temperature ranges.

Received 29th September 2022,
Accepted 8th November 2022

DOI: 10.1039/d2dt03166c

rsc.li/dalton

Introduction

Layered nickel and cobalt hydroxides are important compounds that have attracted much attention in energy storage and catalysis research fields due to their electroactive properties. Both metal(II) hydroxides are used as cathode materials that can readily convert to more oxidised species in a reversible redox reaction in which electron transfer occurs, making them suitable for use in electrochemical applications.¹ Nickel hydroxides have historically been used in rechargeable alkaline batteries such as nickel–cadmium (NiCd) and nickel–metal hydride (NiMH), but have also been studied as corrosion products of nickel–metal alloys and anode materials.² More modern applications of nickel hydroxide include supercapacitors,^{3–5} electrochromic devices such as smart or switchable glass,^{6,7} as well as electroanalysis and electrocatalysis of small organic molecules.⁸ Similarly, cobalt hydroxides are used as catalysts and battery electrode materials, whilst mixed nickel–cobalt hydroxide cathodes often have increased

electrochemical performance and stability compared to the individual metal hydroxides.^{9–11} Cobalt hydroxides are also commonly used in paints, varnishes and printing inks as pigments and drying agents.¹² Impurities in all such phases can be detrimental to their relevant properties.

Two structural polymorphs are reported to exist for the nickel and cobalt hydroxides; a well-defined crystalline beta-phase^{13–16} and a poorly defined alpha-phase.^{17–19} The beta-phases, β -Ni(OH)₂ and β -Co(OH)₂, crystallise with the cadmium iodide (CdI₂) structure and many simple layered hydroxides adopt this structure, including magnesium hydroxide (brucite) and calcium hydroxide (portlandite).²⁰ The layered structure consists of a hexagonal close-packed arrangement of the oxide anions with octahedrally coordinated metal (II) cations and the hydrogen of the hydroxyl anion positioned on a tetrahedral site directed towards the adjacent layer.^{13,16,20} The spectroscopic features and characteristic structure of the alpha-phases, α -Ni(OH)₂ and α -Co(OH)₂, are much less well-defined in the literature, mainly due to difficulties in both their synthesis and characterisation, leading to products which are multiphase and poorly crystalline.

Although corroborating experimental data are sparse, the alpha-phase structures are considered to form through an expansion of the octahedral layers in the *c*-direction of the brucite unit cell; this is hypothesised to occur due to relatively

^aDepartment of Chemistry, Loughborough University, Loughborough, UK.

E-mail: S.E.Dann@lboro.ac.uk

^bSchool of Chemistry, University of Edinburgh, Edinburgh, UK†Electronic supplementary information (ESI) available. See DOI: <https://doi.org/10.1039/d2dt03166c>

weak interactions between the metal hydroxide layers (Fig. S1†). This expansion allows for water and anions to incorporate between the layers and often causes non-ordered stacking of the layers. This has resulted in these hydroxides often being described as ‘turbostratic’ with the nickel analogue being normally amorphous, and the analogous cobalt hydroxide phase typically only showing some partial structural order.^{21–23} The proposed structure of the alpha-phase with negatively charged anions inserted into the gallery space of the brucite-like layers introduces a charge imbalance that is not compensated without oxidation of the divalent cations within the layers or incorporation of counteranions between them.

Layered structures derived from the parent brucite structure, but with anion incorporation, have been previously proposed for the alpha-phase hydroxides.^{21,24–26} Layered double hydroxides (LDHs) and layered hydroxysalts (LHSs) can also both be derived from this simple structure, but the anions incorporate through different mechanisms. A comparison of the different layered hydroxide structures is shown in Fig. 1 which is a schematic highlighting the key differences between the structures. Layered double hydroxides have trivalent cations in the layers as well as anion incorporation on ordered fixed-sites between the layers giving a general formula of $[M^{2+}_{1-x}M^{3+}_x(OH)_2]^{x+}(A^{n-})_{x/n} \cdot yH_2O$. In contrast, in the layered hydroxysalts, the hydroxide anions in the brucite layers have been partially substituted by other anionic species (e.g. nitrate to

form metal hydroxynitrates) that coordinate directly to the metal cations and have the general formula $M(OH)_{2-x}(A^{n-})_{x/n}$ where $x = 0.5, 0.67$ or 1.0 depending on the identity of M (Fig. S2†).

The nickel and cobalt alpha-phase hydroxides are distinct from both of the other layered hydroxide structures that contain anions, due to the much lower amounts of anion present and how the anionic charge is compensated.¹⁹ Unlike the layered double hydroxide-type structures, there is no evidence of trivalent cations in the alpha-phases as both magnetic and X-ray photoelectron spectroscopy (XPS) measurements indicate only divalent ions are present in each case.²⁷ The alpha-phase hydroxides are also typically brightly coloured blue-green (nickel and cobalt) or pink (cobalt) in colour^{19,28–30} suggesting that only divalent cations are present, as mixed-valence nickel and cobalt materials are both brown-black. Layered hydroxysalt-type structures are also a poor match as the anions present in the alpha-phases are held electrostatically in the interlayer space and not covalently bound to the metal cations.³¹ In addition, alpha-phase hydroxides are always hydrated materials whereas anhydrous layered hydroxysalts exist.³¹ Instead, alpha-phase hydroxides are postulated by Kamath and coworkers to have hydrated anions weakly held between the layers similar to the layered double hydroxides/hydroxysalts where $a = 3 \text{ \AA}$ and $c = 23 \text{ \AA}$, but with only metal(II) cations present, similar to the layered hydroxysalts.¹⁹ They hypothesised that the excess negative charge was compensated by itinerant protons that moved freely between the coordinated water molecules intercalated within the layers. This behaviour accounts for the large proton diffusion coefficient of alpha-type hydroxides,¹ facilitating them to act as efficient electrodes in alkaline batteries.¹⁸

Powder X-ray diffraction (PXRD) analysis has been the main method used to characterise the layered hydroxides in the literature to date. While this is useful for beta-phase identification, it has limitations for the detection of small quantities of another phase in the presence of a majority phase, particularly those that are poorly crystalline, such as the alpha-phase hydroxides. This has led to some confusing literature where multiple preparation methods have been used to produce supposedly the same phase but with quite different, and not fully analysed, vibrational spectra.^{32–36} This means the characterisation of these materials is often inconclusive and more detailed analysis of these spectroscopic data is needed to determine the vibrational bands of each individual phase and consequently, the different phases present in mixtures. Variations in the OH:A ratio and the different modes of binding should lead to differences in the band positions and numbers of bands present in each case to allow these data to be used diagnostically.³⁷ Furthermore, the differences between the Raman and infrared spectra can be utilised, along with variations in the decomposition behaviour of each phase, as the strength of binding of the anion differs in each case.

For example, nitrate (NO_3^-) anions present in alpha-phase or layered double hydroxide structures will be hydrated and have three equivalent N–O bonds in a trigonal planar geometry that belongs to the high symmetry D_{3h} point group. In layered

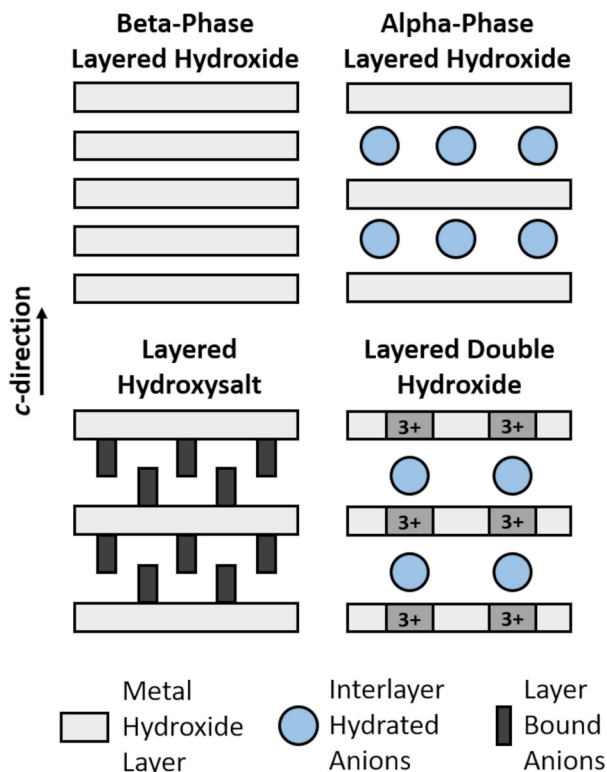


Fig. 1 Diagram of the structural differences between layered hydroxide phases, layered hydroxysalts and layered double hydroxides showing the variations in anion incorporation.



Table 1 The investigated synthesis methods for nickel and cobalt hydroxides and hydroxynitrates with the expected layered hydroxide phases produced

Synthesis method	Expected phase(s)
Chemical precipitation ² – addition of base to a metal(II) salt solution resulting in precipitation.	Alpha-phase or beta-phase layered hydroxides (dependant on conditions).
Electrochemical ^{39,40} – electrochemical reduction of water to hydroxide anions in an aqueous metal(II) salt solution.	Alpha-phase or mixed-phase layered hydroxides (dependant on conditions).
Petrov precipitation ^{32–34} – slow addition of a base solution to a boiling, saturated metal(II) nitrate solution.	Layered hydroxynitrates where $x = 0.5$ or 0.67 .
Metal(II) nitrate thermolysis ⁴¹ – thermal decomposition of the hydrated metal(II) nitrate.	Layered hydroxynitrates where $x = 0.5$ or 0.67 (dependant on the metal).
Mechanochemical ⁴² – pestle and mortar grinding of the hydrated metal(II) nitrate with solid sodium hydroxide.	Layered hydroxynitrates where $x = 0.5, 0.67$ or 1.0 (dependant on the metal).
Evaporation ⁴³ – addition of lithium carbonate to a metal(II) nitrate solution followed by evaporation of the water.	Layered hydroxynitrates where $x = 1.0$.
Urea flux ^{35,36} – thermal decomposition and hydrolysis of urea to form hydroxide anions that react with metal(II) nitrate.	Layered hydroxynitrates where $x = 0.5$ or 0.67 .

hydroxysalt structures, the symmetry of the nitrate anion is reduced to the C_{2v} symmetry point group as direct coordination with the metal(II) cations causes one N–O bond to be different from the other two.³⁸ This difference in symmetry affects the vibrational modes that are observed, with nitrate in D_{3h} symmetry exhibiting four vibrational modes, A'_1 , A''_2 , and $2E'$ (ν_1 to ν_4) with ν_1 being infrared inactive while ν_2 is Raman inactive. When the symmetry is changed to C_{2v} the two doubly degenerate (E') vibrations split resulting in a total of six vibrational bands that are all infrared and Raman active. It is the misinterpretation of these data that has led to discrepancies in the literature where poor characterisation has meant that the same preparative method is reported to produce several different phases.

Here we have investigated the synthetic methods summarised in Table 1 used to prepare layered hydroxide and hydroxynitrate phases in the literature and developed them to provide precise control over the phase formed and consistently isolate single-phase materials. This has resulted in the successful preparation of both nickel and cobalt analogues of the beta-phase and alpha-phase hydroxide polymorphs as well as two different hydroxynitrate phases. These were shown to be phase pure through complementary infrared (IR) and Raman (R) spectroscopy techniques with the observed nitrate anion vibrational frequencies being key for the distinction of these phases. The suitability of urea flux methods for the synthesis of layered hydroxides was also explored by comparing their spectroscopic data with that collected from the pure layered hydroxynitrate phases. This has also highlighted the importance of combining both spectroscopic and thermal methods alongside powder X-ray diffraction to identify different layered hydroxide phases present in any hydroxide material prepared.

Experimental section

Materials

All reagents used were analytical grade and included nickel(II) nitrate hexahydrate (99%, Acros Organics), cobalt(II) nitrate

hexahydrate (99%, ICoNiChem), magnesium(II) nitrate hexahydrate (>99%, Sigma), copper(II) nitrate hemi(pentahydrate) (98%, Alfa Aesar), potassium hydroxide (86%, Fischer Chemical), sodium hydroxide (>97%, Fischer Chemical) and lithium carbonate (>99.9%, Sigma-Aldrich). Ethanol (>99.9%, Fischer Chemical) and propanone (>99.8%, Fischer Chemical) dried over molecular sieves (3 Å) were also used in the preparative methods.

Preparation of nickel and cobalt hydroxides

β -Ni(OH)₂ was prepared by the homogenous chemical precipitation method² where a non-stoichiometric aqueous potassium hydroxide solution (0.25 M, 250 mL) was added slowly to an aqueous nickel(II) nitrate solution (0.25 M, 250 mL). The solution was sealed in a high-density polypropylene (HDPE) bottle and heated for 1 week in an oven at 95 °C. The precipitate that formed was collected by gravity filtration, washed with water (*ca.* 1 L) and dried in an oven at 120 °C for 48 h.

β -Co(OH)₂ could be prepared by a similar method using different reaction conditions where a sodium hydroxide solution (100 mL, 0.5 M) was rapidly added to an aqueous cobalt(II) nitrate solution (20 mL, 1 M). Both solutions were nitrogen purged before the addition was carried out under nitrogen. The solution was stirred at room temperature for 6 h and the bright pink precipitate was collected using a sintered glass crucible (grade 4) under vacuum, washed with ethanol (*ca.* 100 mL) and dried in air.⁴⁴ However, due to the poor long-term stability of the product and as β -Co(OH)₂ is a well-characterised compound, data were also collected on a sample obtained from a commercial supplier (ICoNiChem) which was used without further preparation or purification.

α -Ni(OH)₂ and α -Co(OH)₂ were prepared by the chronopotentiometry electrochemical deposition method.⁴⁵ A three-electrode setup was used that consisted of a fluorine-doped tin oxide (SnO₂:F, FTO) coated glass working electrode ($\sim 13 \Omega \text{ sq}^{-1}$, $5 \times 5 \text{ cm}$, 25 cm^2), a palladium sheet counter electrode ($5 \times 5 \text{ cm}$, 25 cm^2) and a silver–silver chloride reference electrode (Ag|AgCl, 3 M NaCl, $E_0 = +208 \text{ mV}$). A current of -0.1 mA cm^{-1} was applied across the electrodes that were submerged in



an aqueous solution of either nickel(II) nitrate or cobalt(II) nitrate (250 mL, 10 mM) for 15 min. The precipitate (*ca.* 0.5 g) was immediately removed from the electrode and washed with deionised water (*ca.* 25 mL). The product was rapidly dried on a watch glass by decanting the excess water and adding hot propanone (5 mL).

Preparation of nickel and cobalt hydroxynitrates

$\text{Ni}_3(\text{OH})_4(\text{NO}_3)_2$ was prepared by the thermolysis method described by Biswick *et al.*⁴¹ which involved heating nickel(II) nitrate hexahydrate (5.0 g) in an oven at 220 °C for 2 h with stirring every 15 min. The product was washed with anhydrous ethanol (*ca.* 500 mL) to remove any nickel(II) nitrate that remained and dried at 120 °C for 48 h. $\text{Mg}_3(\text{OH})_4(\text{NO}_3)_2$ was also prepared using this method with conditions of 330 °C for 17 h for comparative purposes.

$\text{Co}_3(\text{OH})_4(\text{NO}_3)_2$ was prepared by the precipitation method described by Petrov *et al.*³⁴ where a sodium hydroxide solution (0.50 M) was added dropwise by burette to a stirred solution of cobalt(II) nitrate hexahydrate (3.5 M, 25 mL) heated to >90 °C until the solution pH was 6.0. The addition was performed at less than one drop per second to keep a constant solution volume while heated with care taken to prevent water condensing in the glassware. The final product was washed with propanone (*ca.* 250 mL) and dried at 80 °C for 12 h. $\text{Cu}_2(\text{OH})_3(\text{NO}_3)$ was also prepared for comparative purposes using this method but was washed with water (*ca.* 250 mL) and dried at 120 °C for 48 h.

$\text{Ni}(\text{OH})(\text{NO}_3) \cdot \text{H}_2\text{O}$ was prepared by the solid-state mechanochemical synthesis method outlined by Thomas.⁴² An agate pestle and mortar was heated in an oven set to 120 °C overnight to which nickel(II) nitrate hexahydrate (2.18 g, 7.5 mmol) and solid sodium hydroxide (0.30 g, 7.5 mmol) were added. The reagents were ground together into a uniform paste (*ca.* 2 min) to produce a mixture of the hydroxynitrate phase product and sodium nitrate (nitratine) (Fig. S3(a)†). The sodium nitrate was removed by grinding the sample in hot, anhydrous ethanol (*ca.* 1 L) which was repeatedly decanted with caution taken to prevent the product from drying. The final product was washed with three aliquots of hot propanone (*ca.* 100 mL) and filtered using a hot sintered glass crucible (grade 4) under vacuum.

$\text{Co}(\text{OH})(\text{NO}_3) \cdot \text{H}_2\text{O}$ was prepared by the water evaporation method described by Angelov *et al.*⁴³ where solid lithium carbonate (0.952 g, 12.8 mmol) was added to a stirred 75% cobalt(II) nitrate hexahydrate (7.5 g, 25.8 mmol) solution. The solution was then heated to evaporate the water to obtain a pink product that contained LiNO_3 which was eliminated by washing the product in ethanol (*ca.* 100 mL) followed by hot propanone (*ca.* 30 mL) and dried at 100 °C.

Urea flux preparation of nickel and cobalt hydroxides

The solid-state urea flux synthesis method of nickel and cobalt hydroxysalt phases outlined by Ramesh³⁶ involved a solution of urea (2.0 g) in water (1.2 mL) being added to either nickel(II) nitrate hexahydrate (18.0 g) or cobalt(II) nitrate hexahydrate

(18.0 g). The resultant paste formed was transferred into an oven for 90 min set to 220 °C for the nickel phase and 150 °C for the cobalt phase. The solid product was collected, washed with water (*ca.* 500 mL) then propanone (*ca.* 100 mL) and dried at 120 °C for 48 h.

Nickel(II) and cobalt(II) hydroxyisocyanate phases were prepared using the solution urea flux method outlined by O'Hare *et al.*²⁹ where nickel(II) chloride hexahydrate or cobalt(II) chloride hexahydrate (0.47 g, 10 mM), mannitol (0.03 g, 1 mM), and urea (6.0 g, 500 mM) were dissolved in a nitrogen-purged solution of water (180 mL) and ethanol (20 mL). The addition of the reagent solutions was carried out under nitrogen with magnetic stirring and once the addition was complete the solution was heated at 90 °C for 4 h. The precipitated product was collected using a hot sintered glass crucible (grade 4) under vacuum and washed with water (*ca.* 200 mL), ethanol (*ca.* 100 mL) and propanone (*ca.* 100 mL).

Instrumentation

Powder X-ray diffraction (PXRD) patterns were collected using a Bruker D8 Discover powder diffractometer with $\text{Co K}\alpha_1$ radiation ($\lambda = 1.7889 \text{ \AA}$) selected from a Ge(111) single crystal. The samples were encased between two pieces of amorphous tape and rotated at 30 rpm. The data were collected using a VÅNTEC-1 detector over the range of 10–60° 2 θ and a step size of 0.030°. The International Centre for Diffraction Data (ICDD) powder diffraction file (PDF) database was used for phase identification.

Thermogravimetric analysis (TGA) measurements were carried out using a TA instruments SDT Q600 with sample masses of between 10–20 mg and a reference of alumina (Al_2O_3). A temperature ramp method was used with a heating rate of 5 °C min^{−1} with a gas flow of 100 mL min^{−1}. Nickel samples were heated under nitrogen while cobalt samples were heated under an air atmosphere to avoid the formation of two cobalt oxide decomposition products. The oxide products that formed were verified by powder X-ray diffraction analysis (Fig. S4†).

Microwave plasma-atomic emission spectrometry (MP-AES) elemental analysis was performed by dissolving approximately 100 mg of sample in concentrated nitric acid (68%, 10 mL) and diluting to give cation concentrations in the range 0.1–10 mg L^{−1} (ppm). Solutions were nebulised and introduced to the microwave plasma of the Agilent 4210 MP-AES. The emission wavelengths monitored were 361.939 cm^{−1} for nickel and 340.521 cm^{−1} for cobalt.

Carbon–hydrogen–nitrogen (CHN) elemental analysis was performed by placing approximately 2 mg of sample into a tin capsule and loaded into an Exeter Analytical CE400 Elemental Analysis calibrated with an acetanilide standard.

Infrared (IR) absorption spectra were collected between 4000–250 cm^{−1} using a PerkinElmer Spectrum 100 FT-IR Spectrometer fitted with caesium iodide (CsI) optics. Potassium bromide (KBr) discs were initially used to record the spectra following previous literature methods but the KBr medium was abandoned and replaced with CsI. This was



because KBr reacts with layered hydroxide phases,^{32,46} resulting in nitrate bands at *ca.* 1380 cm⁻¹ in all of the materials analysed regardless of the nitrate anion symmetry present.

Raman (R) data were collected between 4000–100 cm⁻¹ using a Horiba Jobin Yvon HR LabRAM system in the backscatter configuration with a laser line at 633 nm originating from an argon ion laser filtered to 10% power so as not to heat and decompose the sample. The laser was focused onto the sample to a spot size of 1 μm.

Results and discussion

Beta-phase and alpha-phase nickel and cobalt hydroxides

The preparation of green nickel hydroxide was achieved by the chemical precipitation synthesis method. β-Ni(OH)₂ was formed at high temperature over a 7 d duration of chemical ageing and a non-stoichiometric ratio (1 : 1) of the nickel(II) and base reagents. Several cobalt hydroxides could also be made using this method and a blue precipitate initially formed upon addition of the base to the cobalt(II) nitrate solution which would be consistent with α-Co(OH)₂.^{19,23} However, the precipitate when left in the solution readily converted to a mixed-phase pink and purple material. A modified version of this method was also attempted to prepare a single-phase material based on the work by Zeng *et al.*⁴⁴ that involved the rapid addition of a stoichiometric excess of the base solution to the cobalt(II) nitrate solution at room temperature. The precipitate was observed to change from blue to pink and after 6 h of chemical ageing a pink solid could be isolated. Initial powder X-ray diffraction and infrared data collected indicated β-Co(OH)₂ was formed (Fig. S5†). However, this product was not stable and converted to a darker pink-brown colour after several weeks. To avoid confusion in relation to the low stability phase, β-Co(OH)₂ was obtained from a commercial supplier to act as a comparator.

Electrochemical methods formed α-Ni(OH)₂ and α-Co(OH)₂ materials as a film layer deposited onto the electrode surface but difficulties were encountered in attempts to isolate these samples if left damp in air. To ensure isolation of the alpha-phase hydroxides, the product was immediately removed from the electrode, washed with water, followed by the addition of hot propanone that evaporated rapidly to dry the powder. Conventional filtration methods were found to be too slow and allowed conversion to mixtures of phases before analysis could be completed. This was particularly evident in the case of the cobalt hydroxides that changed colour from blue to pink or purple materials while similar observations could not be made for nickel hydroxides as only green coloured materials were encountered.

Fig. 2(a) shows powder X-ray diffraction data collected on the beta-phase and alpha-phase layered hydroxides of nickel and cobalt. The patterns of β-Ni(OH)₂ and β-Co(OH)₂ shown in Fig. 2(a-i) and (a-ii) match to reported data for the nickel hydroxide mineral theophrastrite (ICDD PDF 14-117)⁴⁷ and cobalt hydroxide (ICDD PDF 30-0443)⁴⁸ indicating the brucite-

type structure formed with *a* = 3 Å and *c* = 4.5 Å in space group *P*3̄*m*1. The 001 reflections would be broadened if the layer stacking was disordered, but experimentally they were observed to be as sharp as the other reflections, implying the structures are crystalline. Diffraction patterns of α-Ni(OH)₂ and α-Co(OH)₂ in Fig. 2(a-iii) and (a-iv) were characteristic of amorphous phases with no well-defined reflections observed. This suggests there is very little or no long-range order and indicates the metal hydroxide layers do not have ordered stacking. This is entirely consistent with what is expected for a turbostratic structure.¹³ The features observed at *ca.* 38.5° in α-Ni(OH)₂ and *ca.* 39.0° in α-Co(OH)₂ match the positions of the analogous 100 reflections in the beta-phase diffraction patterns. This reflection is unaffected by the layer stacking that occurs in the *c*-direction of the unit cell and suggests that layers of metal hydroxide are likely formed.²⁴

Thermogravimetric analysis weight loss data in Fig. 2(b) shows that the water lost by dehydroxylation in the two beta-phases occurs over a shorter temperature range (*ca.* *T* = 250–300 °C) in comparison to the alpha-phases where there is a gradual weight loss over a more extended temperature range (*ca.* *T* = 100–350 °C). The beta-phases have observed TGA percentage mass losses that are also congruent with the calculated weight losses of Ni(OH)₂ and Co(OH)₂ to nickel(II) oxide (NiO) and cobalt(II,III) oxide (Co₃O₄) decomposition products. This decomposition occurs over two weight loss steps, first forming disordered cubic metal(II) oxide structures before ordering at higher temperatures with the cobalt phases also oxidising.^{49,50} The TGA mass losses of the alpha-phases are both approximately 3% higher compared to the respective beta-phases. This is consistent with the incorporation of a small portion of hydrated nitrate anions and is shown by the small initial weight loss that occurs before the main dehydroxylation (*ca.* *T* < 220 °C for nickel and *ca.* *T* < 150 °C for cobalt). The phase compositions and degree of anion incorporation in the two alpha-phase hydroxides were determined through a combination of the TGA mass losses and elemental analysis data in Table 2. These TGA datasets could not be carried out in triplicate because of difficulties faced when drying the samples and their rapid conversion into other, mixed-phase materials. These data gave the alpha-phase formula as M(OH)_{1.95}(H₂O)_{0.05}(NO₃)_{0.05} (where M = Ni or Co and *x* = 0.05) which matches with the structural model previously proposed for the alpha-phase hydroxides with a general formula of M(OH)_{2-x}(H₂O)_x(A^{*n*-})_{*x*/*n*} that involves a slight excess of positive charge resulting from 'partial protonation' of the layer hydroxides groups.¹⁹

Infrared and Raman spectra presented in Fig. 2(c) and (d) respectively of the layered hydroxides show several bands that relate to the metal hydroxide lattices. In the beta-phase these include intense O–H stretches at *ca.* 3600–3650 cm⁻¹, O–H bends at *ca.* 490–525 cm⁻¹ as well as *ca.* 250–350 cm⁻¹ and the Ni–O or Co–O lattice mode between *ca.* 430–450 cm⁻¹. In the alpha-phase infrared spectra, the sharp lattice O–H stretches are replaced by broad O–H stretches of water at *ca.* 3500 cm⁻¹ and the water O–H bends are also present at *ca.* 1650 cm⁻¹.³⁷



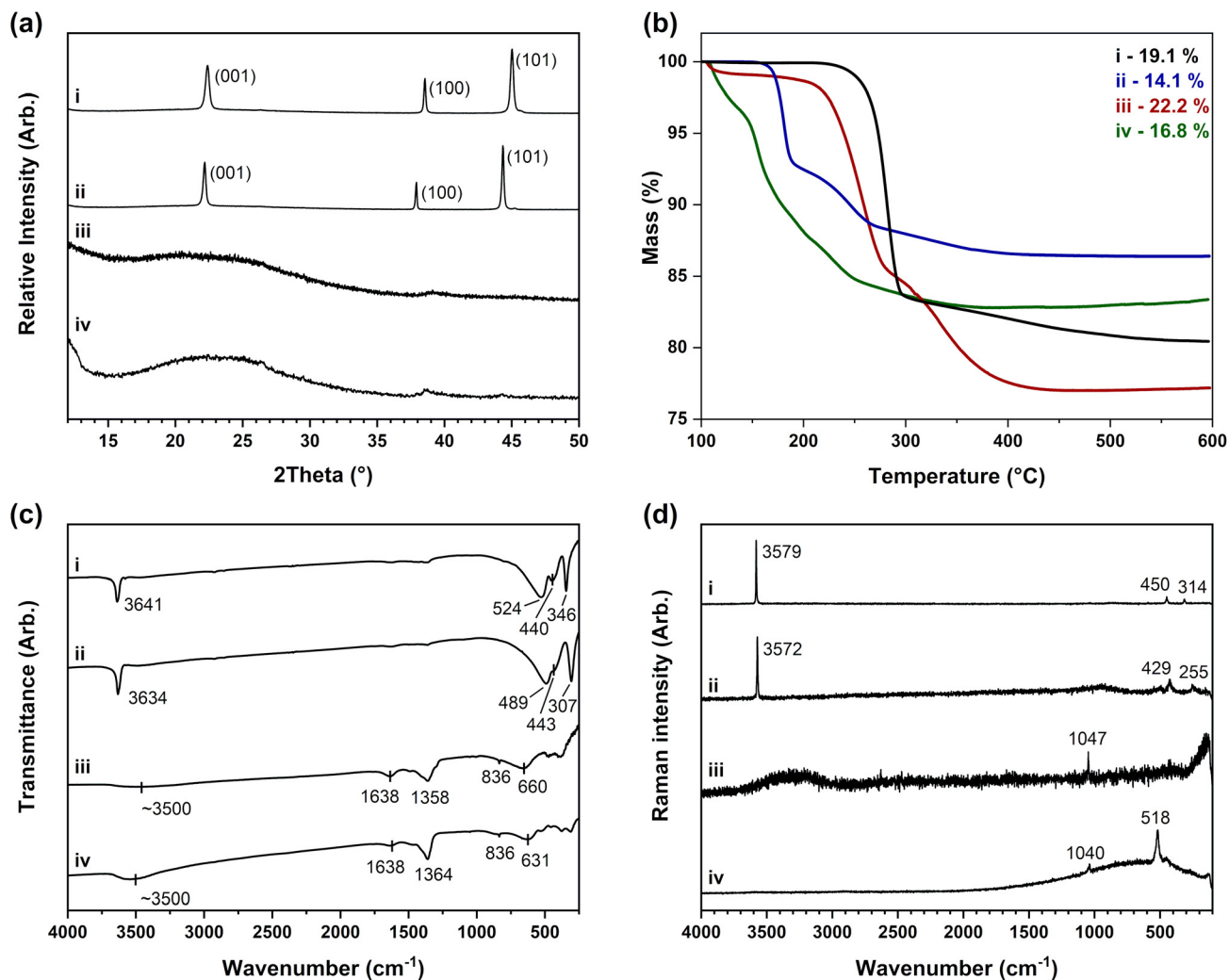


Fig. 2 Data collected of (i) β -Ni(OH)₂, (ii) β -Co(OH)₂, (iii) α -Ni(OH)₂ and (iv) α -Co(OH)₂. (a) Powder X-ray diffraction patterns collected with Co K_{α1} radiation ($\lambda = 1.7889$ Å), (b) thermogravimetric analysis weight loss data with decomposition to NiO and Co₃O₄, (c) infrared absorption spectra as CsI disks and (d) Raman spectra.

Additionally, the alpha-phases have nitrate anions bands present, with three infrared bands at *ca.* 1350 cm⁻¹, 830 cm⁻¹ and 700 cm⁻¹ as well as a Raman band at *ca.* 1050 cm⁻¹. Comparison to the expected reference values identifies the nitrate anions present in alpha-phase layered hydroxides to be in a D_{3h} symmetry, meaning that the anions are hydrated and incorporated between the layers.

Nickel and cobalt layered hydroxynitrates

Several experimental procedures for the preparation of layered hydroxynitrates were used, resulting in the synthesis of two nickel and two cobalt hydroxynitrate phases. The precipitation method described in the work by Petrov *et al.*^{32,34} suggested that the phases Ni₂(OH)₃(NO₃) and Co₂(OH)₃(NO₃) where $x = 0.5$ were formed,⁵¹ however, the use of this method initially formed mixed-phased nickel or cobalt hydroxides. A single-phase cobalt hydroxynitrate material was successfully prepared by altering the method to a very slow addition of the base to

the cobalt(II) nitrate. Rapid addition caused dilution of the solution and led to a blue phase being formed that is likely an α -Co(OH)₂. Pink β -Co(OH)₂ was also observed in the mixed-phase materials when the base addition exceeded pH 6.0 and this was confirmed by analysis of powder X-ray diffraction data collected at intervals of base addition (Fig. S6†).

The thermolysis method that involves heating the hydrated metal(II) nitrates in an oven for 12 h was used by Biswick *et al.*⁴¹ to prepare Ni₂(OH)₃(NO₃), Cu₂(OH)₃(NO₃), Mg₂(OH)₃(NO₃) and Zn₃(OH)₄(NO₃)₂ at 220 °C, 150 °C, 330 °C and 170 °C respectively. Using the specified conditions for the nickel hydroxynitrate phase resulted in decomposition to nickel(II) oxide. Successful phase formation instead required a significantly reduced heating time of only 2 h. This produced the desired phase with some remaining nickel(II) nitrate hexahydrate that could be washed out with water without affecting the nickel hydroxynitrate phase. This method was also attempted with cobalt(II) nitrate but cobalt(II,III) oxide was

Table 2 Elemental and thermogravimetric analysis of the prepared layered hydroxide and hydroxysalt phases. The error of % M is given while for % C, % H, and % N is $\pm 0.3\%$

	Elemental analysis (MP-AES/CHN)								Thermogravimetric analysis (TGA)		
	Theoretical values				Experimental values				End phase	Theoretical mass losses (%)	Experimental mass losses (%)
	% M	% C	% H	% N	% M	% C	% H	% N			
β -Ni(OH) ₂ (precipitation)	63.3	0.0	2.1	0.0	65.2 (± 1.3)	0.2	1.9	0.0	NiO	19.4	19.1 (± 0.2)
α -Ni(OH) ₂ (electrochemical)	61.2	0.0	2.2	0.7	64.0 (± 0.1)	0.4	1.9	0.9	NiO	22.1	22.2
Ni ₃ (OH) ₄ (NO ₃) ₂ (thermolysis)	47.8	0.0	1.1	7.6	47.0 (± 0.8)	0.1	1.0	6.7	NiO	39.1	37.9 (± 0.3)
Ni(OH)(NO ₃)·H ₂ O (mechanochemical)	37.7	0.0	2.0	9.0	39.7 (± 1.0)	0.4	1.9	8.2	NiO	52.1	51.9 (± 0.8)
Ni ₃ (OH) ₄ (NO ₃) _{1.9} (OCN) _{0.1} (solid-state urea flux)	48.1	0.3	1.1	7.7	54.9 (± 0.8)	0.2	1.3	6.4	NiO	38.8	38.4 (± 0.1)
Ni ₂ (OH) ₃ (OCN)·H ₂ O (solution urea flux)	51.4	5.3	2.2	6.2	51.2 (± 0.5)	5.9	1.5	5.6	NiO	34.6	34.0 (± 0.6)
β -Co(OH) ₂ (commercial reagent)	63.4	0.0	2.1	0.0	61.5 (± 2.8)	0.4	2.0	0.1	Co ₃ O ₄	13.5	14.1 (± 0.6)
α -Co(OH) ₂ (electrochemical)	61.3	0.0	2.2	0.7	58.2 (± 2.4)	0.5	2.0	0.6	Co ₃ O ₄	16.3	16.8
Co ₃ (OH) ₄ (NO ₃) ₂ (Petrov precipitation)	47.9	0.0	1.1	7.6	52.0 (± 1.6)	0.1	1.1	6.5	Co ₃ O ₄	34.7	29.5 (± 0.9)
Co(OH)(NO ₃)·H ₂ O (evaporation)	37.8	0.0	1.9	9.0	38.3 (± 1.1)	0.1	1.8	7.8	Co ₃ O ₄	48.6	47.1 (± 0.1)
Co ₃ (OH) ₄ (NO ₃) _{1.9} (OCN) _{0.1} (solid-state urea flux)	48.2	0.3	1.1	7.7	50.7 (± 1.0)	0.3	1.3	5.8	Co ₃ O ₄	34.4	32.3 (± 0.1)
Co ₂ (OH) ₃ (OCN)·H ₂ O (solution urea flux)	51.5	5.3	2.2	6.2	53.0 (± 1.9)	6.6	1.3	6.9	Co ₃ O ₄	29.9	24.5 (± 1.4)

formed despite the use of lower temperatures and with shorter durations.

The powder X-ray diffraction patterns collected for the nickel hydroxynitrate phase prepared by the thermolysis method in Fig. 3(a-i) and the cobalt hydroxynitrate phase prepared by the Petrov methods in Fig. 3(a-ii) show the two phases are similar, with both exhibiting anisotropic broadening of all the reflections observed. The positions of these reflections can be matched to literature data of several hydroxynitrate phases with different stated compositions, including literature datasets of Ni₂(OH)₃(NO₃) and Co₂(OH)₃(NO₃) (where $x = 0.5$)^{32–34} as well as Ni₃(OH)₄(NO₃)₂,⁵² Zn₃(OH)₄(NO₃)₂,⁵³ and Mg₃(OH)₄(NO₃)₂⁵⁴ (where $x = 0.67$) (Fig. S7†).

The mechanochemical synthesis method was used by Thomas⁴² to prepare layered hydroxynitrates with formulae of Cu₂(OH)₃(NO₃) and Cd₂(OH)₃(NO₃) as well as a poorly crystalline nickel phase that formed after washing with water and was quoted to be an alpha-phase hydroxide. Repeating this methodology for nickel and cobalt hydroxynitrates initially produced mixed-phase layered hydroxides, however, a single-phase nickel material was produced by altering the method. The reaction was instead performed at a higher temperature, achieved using a hot pestle and mortar, to avoid conversion to other phases by discouraging excess water uptake by the targeted phase. Washing to remove the sodium nitrate by-product was performed using ethanol dried over molecular sieves in place of water. The metal(II) nitrate and sodium hydroxide reagent proportions were also changed from a 10 : 6 ratio to a 1 : 1 ratio to reflect the phase composition produced.

The diffraction pattern of the cobalt hydroxynitrate phase prepared by this updated procedure had several additional reflections observed that were not present in the diffraction data collected before the sodium nitrate impurity was removed (Fig. S3(b)†). To overcome the issues with removing the sodium nitrate impurity from this sample, the water evaporation method proposed by Angelov *et al.*⁴³ which uses lithium carbonate as a starting reagent was carried out to synthesise a pure cobalt phase.

Powder X-ray diffraction analysis of nickel hydroxynitrate mechanochemically prepared in Fig. 3(a-iii) and the cobalt hydroxynitrate prepared by the evaporation method in Fig. 3(a-iv) are similar to one another. These diffraction patterns match well to the reported datasets of Ni(OH)(NO₃)·H₂O (ICDD PDF 27-939)⁵⁵ and Co(OH)(NO₃)·H₂O⁵⁶ which are considered to be isostructural with Zn(OH)(NO₃)·H₂O that forms with better crystallinity and has a determined structure reported by Louër,^{55,57} crystallising with the monoclinic unit cell (where $a = 18 \text{ \AA}$, $b = 3 \text{ \AA}$, $c = 14 \text{ \AA}$) and $P2_1/c$ space group.

The compositions of the Co and Ni layered hydroxynitrates were determined through analysis of elemental and thermogravimetric data as presented in Table 2 with the TGA weight loss curves shown in Fig. 3(b). The nickel phase prepared by the thermolysis methods and the cobalt phase by the Petrov precipitation were determined to have the formula M₃(OH)₄(NO₃)₂ (where M = Ni, Co) with $x = 0.67$. It is noted that the TGA weight loss of $29.5 \pm 0.9\%$ is not within the ESD of the expected value of 34.7% for the cobalt phase. This discrepancy is assumed to be due to inconsistencies seen during the oxidation of the cobalt hydroxynitrate phases in air to Co(II) and Co(III) with CoO forming as well as Co₃O₄ even on prolonged heating. As a result, cobalt gravimetric analysis was also carried out using the method described by Upadhyaya *et al.*⁵⁸ (Table S1†). The results elicit a cobalt content that is $3.7 \pm 0.9\%$ lower than expected, however, this is a systematic error also observed with the cobalt sulfate hexahydrate standard suggesting that assignment of the $x = 0.67$ phase is reasonable when coupled with the vibrational data. The weight loss steps observed in both Fig. 3(b-i) and (b-ii) indicates the decomposition of the nitrate and hydroxide anions occurs simultaneously. In contrast to this, the data of the Ni(OH)(NO₃)·H₂O and Co(OH)(NO₃)·H₂O phases in Fig. 3(b-iii) and (b-iv) show two weight loss steps. The first step is 18% in the nickel phase (*ca.* $T = 105\text{--}245 \text{ }^\circ\text{C}$) and 11% in the cobalt phase (*ca.* $T = 110\text{--}160 \text{ }^\circ\text{C}$). This relates to the loss of the hydrated water as well as the water from the decomposition of the hydroxide anions. The final weight losses then equate to the



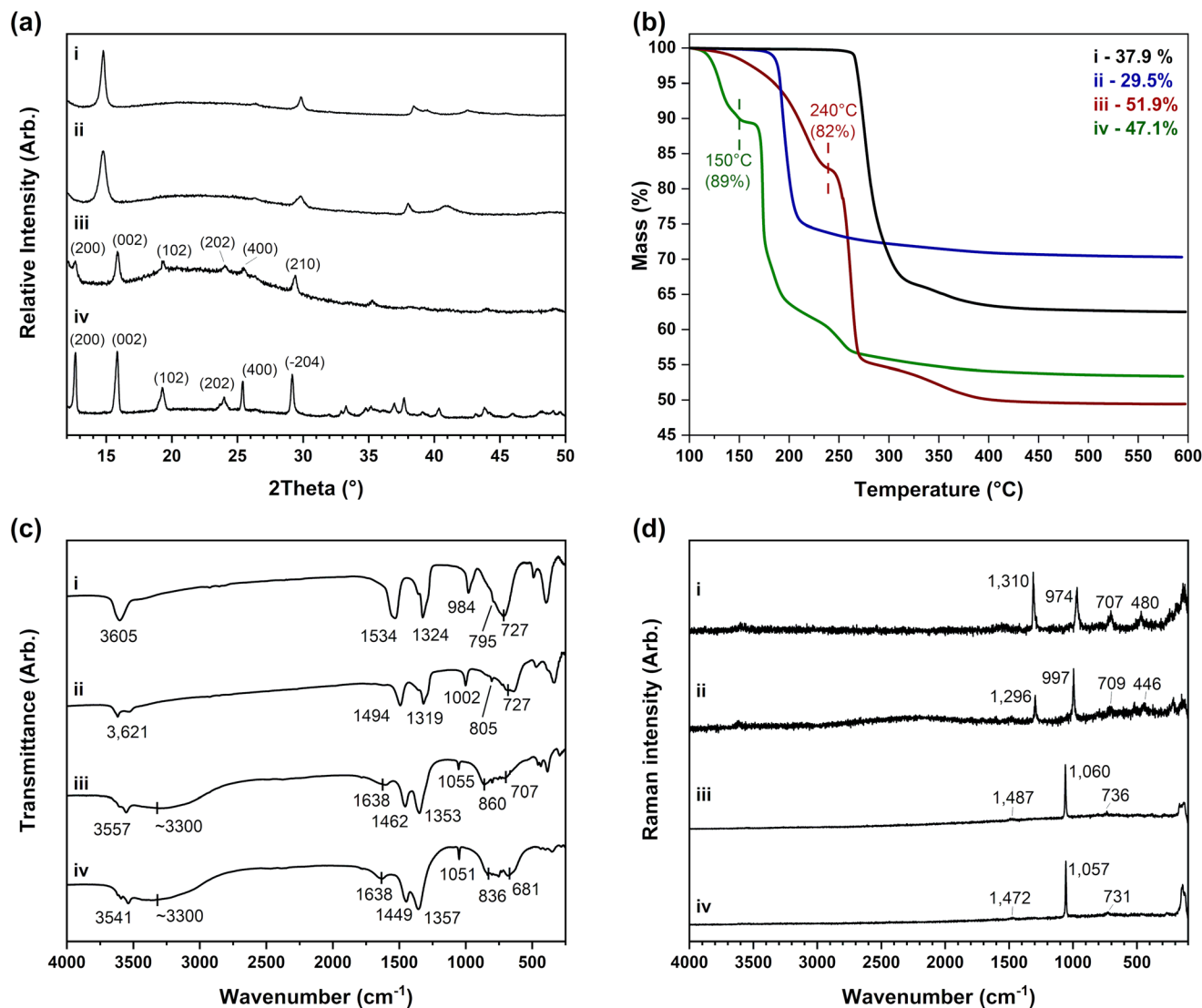


Fig. 3 Data collected of (i) $\text{Ni}_3(\text{OH})_4(\text{NO}_3)_2$, (ii) $\text{Co}_3(\text{OH})_4(\text{NO}_3)_2$, (iii) $\text{Ni}(\text{OH})(\text{NO}_3)\cdot\text{H}_2\text{O}$ and (iv) $\text{Co}(\text{OH})(\text{NO}_3)\cdot\text{H}_2\text{O}$. (a) Powder X-ray diffraction patterns collected with Co $K_{\alpha 1}$ radiation ($\lambda = 1.7889 \text{ \AA}$), (b) thermogravimetric analysis weight loss data with decomposition to NiO and Co_3O_4 , (c) infrared absorption spectra as CsI disks and (d) Raman spectra.

decomposition of the nitrate anions with subsequent formation of nickel(II) oxide and cobalt(II,III) oxides similar to the decomposition of the other layered hydroxide phases. Therefore, the hydration of the $\text{M}(\text{OH})(\text{NO}_3)\cdot\text{H}_2\text{O}$ phases causes the additional water lost by the dehydroxylation reactions to occur at a lower temperature in contrast to the anhydrous $\text{M}_3(\text{OH})_4(\text{NO}_3)_2$ (where $\text{M} = \text{Ni}, \text{Co}$) phases where the weight loss from the dehydroxylation and nitrate decomposition occurs simultaneously.

Infrared spectra in Fig. 3(c) of the layered hydroxynitrates show that the $\text{M}(\text{OH})(\text{NO}_3)\cdot\text{H}_2\text{O}$ phases in Fig. 3(c-iii) and (c-iv) are hydrated with the O–H stretches of water at $\text{ca. } 3500 \text{ cm}^{-1}$ and O–H bends at $\text{ca. } 1650 \text{ cm}^{-1}$ whereas these water bands are not present in the $\text{M}_3(\text{OH})_4(\text{NO}_3)_2$ phases. Bands of the nitrate anions are also present at $\text{ca. } 1450, 1350, 1050, 850$ and 700 cm^{-1} in the infrared data. Through analysis of the infrared

bands as well as the bands at $\text{ca. } 1480, 1060$ and 730 cm^{-1} in the Raman spectra in Fig. 3(d) it can be determined the anions have C_{2v} symmetry. This is because the nitrates are coordinated to the metal(II) cations directly and are different to the hydrated nitrate anions incorporated between the layers observed in the alpha-phase hydroxides that had D_{3h} symmetry.

The two hydroxynitrate compositions can be distinguished by key differences in the nitrate bands observed. The first is the position of the symmetric N–O stretch between $974\text{--}1002 \text{ cm}^{-1}$ in $\text{M}_3(\text{OH})_4(\text{NO}_3)_2$ but $1051\text{--}1060 \text{ cm}^{-1}$ in $\text{M}(\text{OH})(\text{NO}_3)\cdot\text{H}_2\text{O}$. The second is the relative splitting of the two symmetric stretching bands that lie in the region between $1300\text{--}1600 \text{ cm}^{-1}$ formed from the loss of the double degeneracy of D_{3h} nitrate. For example, these infrared bands are separated by 210 cm^{-1} and 175 cm^{-1} in $\text{Ni}_3(\text{OH})_4(\text{NO}_3)_2$ and

$\text{Co}_3(\text{OH})_4(\text{NO}_3)_2$ respectively, whereas they are only separated by 109 cm^{-1} and 92 cm^{-1} for $\text{Ni}(\text{OH})(\text{NO}_3)\cdot\text{H}_2\text{O}$ and $\text{Co}(\text{OH})(\text{NO}_3)\cdot\text{H}_2\text{O}$, respectively. These are characteristic features of the layered hydroxynitrate compositions and will allow for them to be distinguished from one another as well as other layered hydroxide phases.

Spectroscopic phase identification

The use of spectroscopic infrared and Raman methods to distinguish between the different layered hydroxide and layered hydroxynitrate phases has been demonstrated as a method of determining the layered hydroxide phases formed, particularly in mixed-phase materials. This is made possible by the changes in symmetry of the nitrate ions and Table 3 summarises the data from the different phases studied.

The spectra of $\beta\text{-Ni}(\text{OH})_2$ and $\beta\text{-Co}(\text{OH})_2$ show only intense absorption bands present that relate to the lattice hydroxide anions as well as the Ni–O and Co–O lattice modes with no evidence of water or nitrate anions being present. The sharp lattice hydroxide band at *ca.* 3650 cm^{-1} is characteristic of the beta-phase and can be used for identification. The spectra collected on samples of $\alpha\text{-Ni}(\text{OH})_2$ and $\alpha\text{-Co}(\text{OH})_2$ show a broad O–H stretch present at *ca.* 3500 cm^{-1} which is characteristic of the phase but is not specific to the alpha-phases as this would also be present in any hydrated phases.

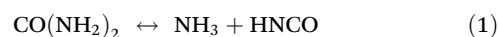
The nitrate anions incorporated in the alpha-phase have a D_{3h} symmetry which has a characteristic band at *ca.* 1350 cm^{-1} , however, upon the band splitting due to the loss of degeneracy when changed to a C_{2v} symmetry of a hydroxynitrate phase, the bands of the two symmetries can overlap. The symmetric stretch band between 990 and 1050 cm^{-1} is not infrared active in a D_{3h} symmetry but is infrared active in C_{2v} symmetry. Therefore, the presence of this band in an infrared

spectrum is diagnostic of covalent nitrate anions and the specific presence of hydroxynitrate phases, not simply just nitrate anions present in an alpha-phase or disordered beta-phase hydroxide as reported in many previous studies.^{25,26,62,63}

Raman spectroscopy can also be used to deduce the exact band position which is specific to the phase present and varies between the different layered hydroxysalts. For example, a band at *ca.* 1050 cm^{-1} would suggest the $\text{M}(\text{OH})(\text{NO}_3)\cdot\text{H}_2\text{O}$ phase while the band at *ca.* 1000 cm^{-1} would imply the $\text{M}_3(\text{OH})_4(\text{NO}_3)_2$ phase. Additionally, the metal(II) nitrate hexahydrate starting materials can be distinguished from the layered hydroxide and hydroxynitrate phases through the precise position of this band obtained by Raman spectroscopy (Fig. S8†). Furthermore, the $\text{M}_3(\text{OH})_4(\text{NO}_3)_2$ formula determined (where M = Ni or Co) are also suggested to be correct as the infrared band splitting observed for the phases are closer to 163 cm^{-1} of $\text{Mg}_3(\text{OH})_4(\text{NO}_3)_2$ where $x = 0.67$ than the smaller 70 cm^{-1} of $\text{Cu}_2(\text{OH})_3(\text{NO}_3)$ where $x = 0.5$ (Fig. S9†). The symmetric N–O stretch of nitrate in the Raman data at 974 cm^{-1} in the nickel phase and 997 cm^{-1} in the cobalt phase are also closer to the magnesium phase which is at 1004 cm^{-1} than the copper phase at 1049 cm^{-1} .

Urea flux preparation methods of nickel and cobalt hydroxides

Layered hydroxynitrate synthesis methods involving the addition of urea are thought to give greater control over the phase formation while also increasing the phase crystallinity.³⁵ Urea pyrolyses when heated above $70\text{ }^\circ\text{C}$ according to the eqn (1) shown below.



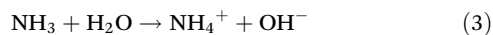
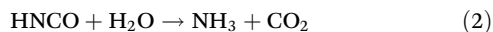
If water is present, subsequent hydrolysis reactions occur upon cyanic acid formation, eventually leading to the pro-

Table 3 Assignment of the observed nitrate infrared and Raman bands for the nickel and cobalt layered hydroxides and hydroxynitrates compared to reported values expected for nitrate in a D_{3h} and C_{2v} symmetry^{38,59–61} as well as to the metal(II) nitrate hexahydrate starting reagents and similar metal hydroxynitrates

	Nitrate anion vibrational modes (cm^{-1})							
	ν_1		ν_2		ν_3		ν_4	
	Symmetric stretch (ν_s)		Out-of-plane bend (γ)		Asymmetric stretch (ν_{as})		In-plane bend (δ)	
Ref. bands (D_{3h} symmetry)	1050 (A'_1) (R only)		830 (A''_2) (IR only)		1350 (E')		715 (E')	
Ref. bands (C_{2v} symmetry)	1000 (A_1)		800 (B_1)		1290 (A_1), 1400–1500 (B_2)		740 (A_1), 715 (B_2)	
	IR	R	IR	R	IR	R	IR	R
$\beta\text{-Ni}(\text{OH})_2$	—	—	—	—	—	—	—	—
$\alpha\text{-Ni}(\text{OH})_2$	—	1047	833	—	1358	—	628	—
$\text{Ni}_3(\text{OH})_4(\text{NO}_3)_2$	984	974	795	796	1324, 1534	1310, ~1546	—, 727	707, —
$\text{Ni}(\text{OH})(\text{NO}_3)\cdot\text{H}_2\text{O}$	1055	1060	860	—	1353, 1462	—, 1487	803, 707	736, —
$\text{Ni}(\text{NO}_3)_2\cdot 6\text{H}_2\text{O}$	1048	1057	835	—	1349, —	1375, —	—, 659	732, 703
$\beta\text{-Co}(\text{OH})_2$	—	—	—	—	—	—	—	—
$\alpha\text{-Co}(\text{OH})_2$	—	1040	863	—	1350	—	631	—
$\text{Co}_3(\text{OH})_4(\text{NO}_3)_2$	1002	997	805	815	1319, 1494	1296, 1489	727, 655	709, 518
$\text{Co}(\text{OH})(\text{NO}_3)\cdot\text{H}_2\text{O}$	1051	1057	836	—	1357, 1449	—, 1472	755, 681	731, —
$\text{Co}(\text{NO}_3)_2\cdot 6\text{H}_2\text{O}$	1049	1060	834	—	1358, —	1362, —	—, 681	731, —
$\text{Mg}_3(\text{OH})_4(\text{NO}_3)_2$	1014	1004	799	—	1334, 1497	1331, —	733, 711	733, —
$\text{Cu}_2(\text{OH})_3(\text{NO}_3)$	1048	1049	886	—	1353, 1423	1326, —	783, 677	722, 713



duction of hydroxide anions from the uptake of H^+ as ammonium ions, as shown in eqn (2) and (3).³⁶



A solid-state urea flux method, similar to the thermolysis method, is described in the literature with both $\text{Co}_2(\text{OH})_3(\text{NO}_3)^{64}$ and $\text{Co}_3(\text{OH})_4(\text{NO}_3)_2^{65}$ compositions quoted to be formed. Infrared spectra presented in these studies suggest cyanate anions are also incorporated, so a solution urea flux method²⁹ for the preparation of layered hydroxyisocyanate phases of formula $\text{M}_2(\text{OH})_3(\text{OCN})$ was also utilised to synthesise both a reported Co, and unknown Ni, analogue.

Powder X-ray diffraction patterns of the materials synthesised using the solid-state urea flux method are shown in Fig. 4(a-i) and (a-ii) and indicate the phases formed have good

crystallinity. This is established as the reflections are sharper and more intense than the reflections present in the diffraction patterns of the $\text{M}_3(\text{OH})_4(\text{NO}_3)_2$ (where $\text{M} = \text{Ni}$ or Co) in Fig. 3(a-i) and (a-ii) prepared by the previously described methods. The data shown in Fig. 4(a-iii) and (a-iv) for the solution method show poorer crystallinity but match closely to the cobalt hydroxide phase with cyanate anions prepared by O'Hare *et al.*²⁹ which was refined on an $R\bar{3}m$ hexagonal unit cell (where $a = 3 \text{ \AA}$ and $c = 23 \text{ \AA}$). These cell parameters are characteristic of a hydrotalcite-type or alpha-type phase. The analogous nickel phase included here has not been previously reported in the literature. Fig. 4(b) shows the thermogravimetric analysis curves of these four phases which show that the decomposition of hydroxide and any intercalated nitrate and cyanate anions occurs simultaneously.

Infrared and Raman spectra in Fig. 4(c) and (d) of the hydroxynitrate materials prepared using the urea flux method

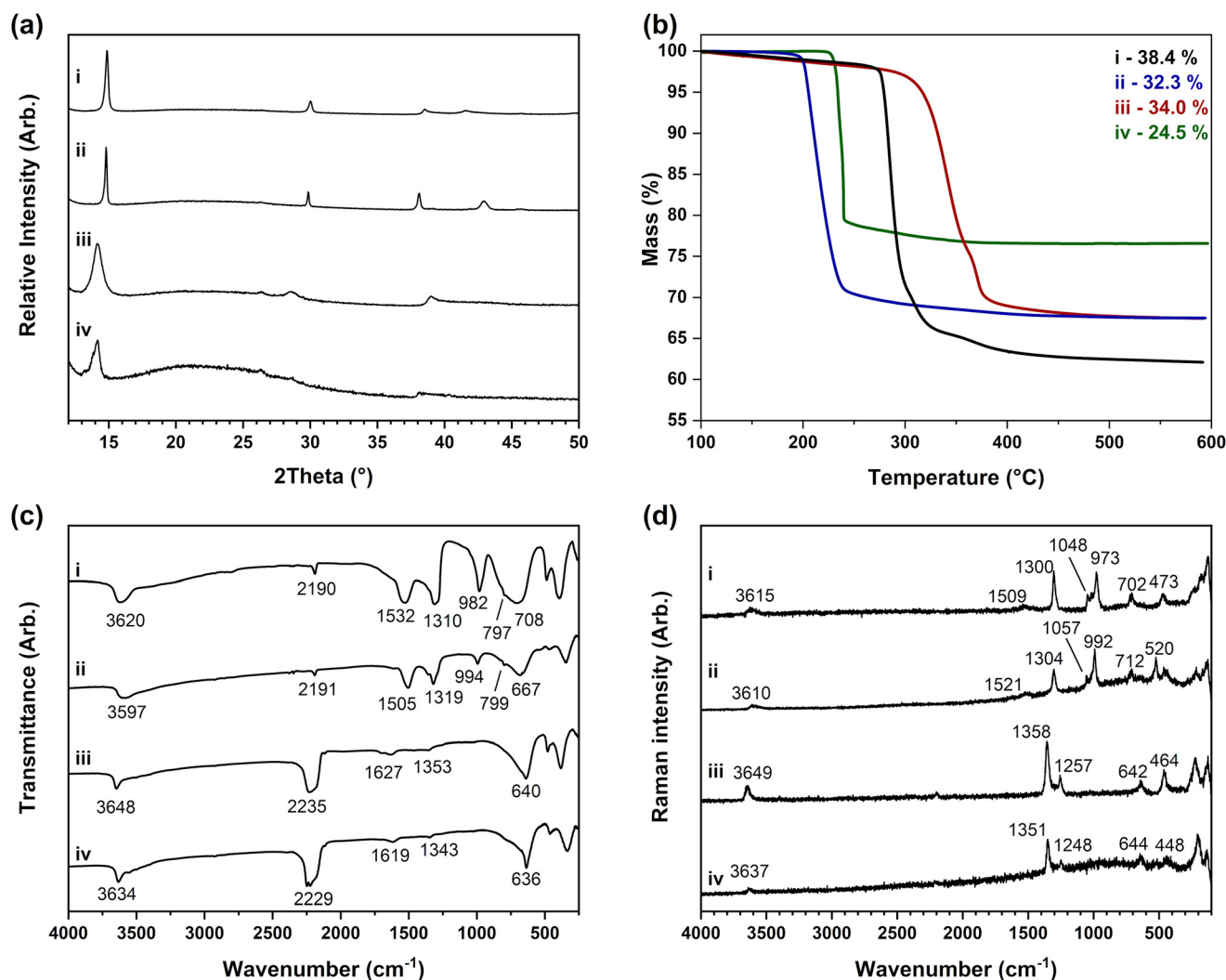


Fig. 4 Data collected of (i) nickel hydroxysalt and (ii) cobalt hydroxysalt prepared by solid-state urea flux methods as well as (iii) nickel hydroxyisocyanate and (iv) cobalt hydroxyisocyanate prepared by solution urea flux methods. (a) Powder X-ray diffraction patterns collected with $\text{Co K}_{\alpha 1}$ radiation ($\lambda = 1.7889 \text{ \AA}$), (b) thermogravimetric analysis weight loss data with decomposition to NiO and Co_3O_4 , (c) infrared absorption spectra as CsI disks and (d) Raman spectra.

of Ramesh and coworkers indicate the presence of cyanate anions in the phase with a band at *ca.* 2200 cm⁻¹. These cyanate anions are available to incorporate into the structure as the cyanic acid (HNCO) formed through the pyrolysis of urea is not fully hydrolysed during the synthesis. Nitrate anion bands are additionally present in the datasets of materials prepared by the solid-state urea flux method shown in Fig. 4(c-i), (c-ii), (d-i) and (d-ii). These bands were also present in the data published for these phases prepared by Ramesh and suggest these are mixed-anion materials with both nitrate and isocyanate incorporated into the structure. This compositional discrepancy may have caused the previous confusion where samples prepared by Ramesh using this method had both Co₂(OH)₃(NO₃)⁶⁴ and Co₃(OH)₄(NO₃)₂ compositions assigned in different publications.^{36,64,65}

The exact formulae of the nickel and cobalt hydroxysalt materials prepared by the solid-state urea flux method cannot be determined with certainty from the TGA data alone. Using the theoretical values listed in Table 4, the total weight loss of 38.4% for the nickel phase is closest to the Ni₃(OH)₄(NO₃)₂ composition (where *x* = 0.67) while the 32.3% for the cobalt phase is between the Co₃(OH)₄(NO₃)₂ (where *x* = 0.67) and Co₂(OH)₃(NO₃) compositions. However, these formulae do not account for the presence of cyanate anions. Combining this information with the elemental analysis data, the compositions can be recalculated as M₃(OH)₄(NO₃)_{1.9}(OCN)_{0.1} which matches with the M₃(OH)₄(NO₃)₂ phase (where M = Ni, Co and *x* = 0.67). Despite this, the observed TGA mass loss for the cobalt phase is 2.1% lower than the theoretical value for the suggested phase, a difference that is not seen for the equivalent nickel phase. It is, therefore, again suspected that inconsistencies are being seen in the oxidation of cobalt phases in air, as observed earlier for cobalt hydroxynitrates. This hypothesis is further supported by the similar position of the nitrate bands in these phases compared to those of the nickel and cobalt hydroxynitrates prepared by the Petrov (for Co) and thermolysis (for Ni) methods which have the chemical formula, M₃(OH)₄(NO₃)₂ as shown in Table 3.

In contrast, materials prepared by the solution urea flux method contain only cyanate anions, as indicated by the infrared spectra in Fig. 4(c-iii) and (c-iv) which show only a broad cyanate band at 2227 cm⁻¹. In the first instance, hydrated M₂(OH)₃(OCN) (where M = Ni, Co and *x* = 0.5) formulae are determined from both thermogravimetric and elemental analysis data listed in Table 2. This is the same formula deter-

mined for the cobalt hydroxyisocyanate phase prepared using this method by O'Hare *et al.*²⁹ where the authors assign the phase as a layered hydroxyisocyanate because almost all of the first-row transition metals form divalent N-bonded isocyanate complexes.

However, the cyanate band observed at 2227 cm⁻¹ in Fig. 4 (c-iii) and (c-iv) is broadened in contrast to the sharp and weak band at the lower wavenumber 2195 cm⁻¹ observed in spectra collected on the materials prepared by the solid-state urea flux method in Fig. 4(c-i) and (c-ii). This is similar to the anion bands of hydrotalcite-type materials that are broadened due to the formation of weakly coordinated anion within the layer structure. From these data, it is proposed that the phases prepared in urea solution are alpha-like layered phases where hydrated cyanate anions are weakly coordinated, rather than a true hydroxysalt phase where the anions are normally more strongly bonded with sharp infrared absorptions. The Ni and Co phases have closely related formulae and could be rearranged into a more alpha-phase type formula of M(OH)_{1.5}(OCN)_{0.5}·H₂O, although it is accepted that the level of anion incorporation is unusually high for an alpha-phase and some compositional variation (anion incorporation and hydration) is expected to be observed for alpha-phases. Despite the identification of more than one OCN phase, a similar spectroscopic approach used for identifying mixtures of the nitrate-based phases described in this study is not possible with the linear cyanate anions; neither significant wavenumber shifts nor splitting is observed, only sharpening of the band on incorporation of the OCN in the hydroxyl layers.

Analysis of mixed-phase layered hydroxides

This work has highlighted the complexities involved when studying layered hydroxide compounds, particularly that multiple characterisation methods are needed to unequivocally identify the key layered hydroxide phases, particularly in cases where the materials produced are mixed-phase. Due to the poorly crystalline nature of mixed-phase materials where any long-range order of the individual phases is reduced, it is not sufficient to identify the phases through powder X-ray diffraction techniques alone, which is normally the technique of choice for a materials chemist or physicist. Spectroscopic and thermal techniques in tandem with powder X-ray diffraction data are a more robust approach for distinguishing and identifying the phases present based on the environment of the incorporated nitrate anion and differences in decomposition temperatures. Nonetheless, even this is limited to cases where certain reagents are used, *e.g.* metal(II) nitrates, and it may not be possible when using other starting materials, such as metal (II) halides. When considering all the above points, it is clear why there are so many discrepancies and uncertainties in the identification of layered hydroxide phases as published in the literature.^{32–34} The revised and refined synthetic methods presented in this work should allow single-phase materials of targeted compositions to be consistently synthesised and impurities to be identified.

Table 4 The theoretical total TGA weight losses of the nickel and cobalt layered hydroxynitrate phases where *x* = 0.5, 0.67 and 1.0

Layered hydroxynitrate	Expected TGA weight losses (%)	
	M = Ni	M = Co
M ₂ (OH) ₃ (NO ₃) (where <i>x</i> = 0.5)	35.2	30.5
M ₃ (OH) ₄ (NO ₃) ₂ (where <i>x</i> = 0.67)	39.1	34.7
M(OH)(NO ₃)·H ₂ O (where <i>x</i> = 1.0)	52.1	48.6



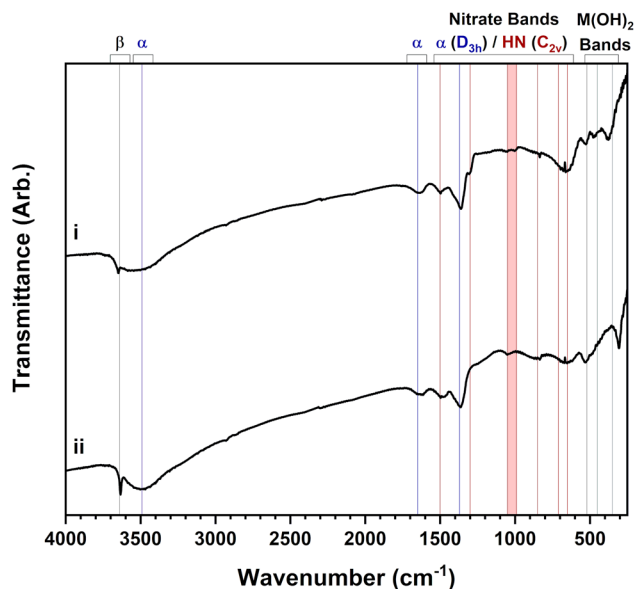


Fig. 5 Infrared absorption spectra data collected as CsI disks of mixed-phase (i) nickel hydroxides and (ii) cobalt hydroxides prepared by electrochemical deposition techniques. Four different layered hydroxide phases are identified including the beta-phase and alpha-phase hydroxides as well as two hydroxynitrate phases evidenced by the two nitrate symmetric stretch bands at ca. 1000 cm⁻¹.

The extensive materials characterisation carried out on this set of materials will provide valuable reference data for the study of layered hydroxides and can be used to confirm whether samples are truly single-phase or contain additional closely-related impurity phases. For example, the infrared spectra presented in Fig. 5 show aged mixed-phase nickel and cobalt hydroxides formed using the electrochemical method. These samples were amorphous to powder X-ray diffraction techniques and their impurities, invisible. Using the values listed in Table 3, it is possible to identify 4 phases in the samples. The beta-phase hydroxide is implicated by the sharp hydroxyl band at ca. 3650 cm⁻¹ as well as the alpha phase expected to be produced by electrochemical method; bands are present at ca. 3500 cm⁻¹, 1650 cm⁻¹ and 1360 cm⁻¹ that indicate hydrated nitrate anions in a D_{3h} symmetry. In addition, both layered hydroxynitrate phases are also present as confirmed by the presence of characteristic bands of nitrate with C_{2v} symmetry; symmetric stretching bands at both ca. 1050 cm⁻¹ ($x = 1.0$) and ca. 1000 cm⁻¹ ($x = 0.67$) indicate the two different hydroxynitrates.

Conclusions

Methods identified in the literature for the preparation of nickel and cobalt layered hydroxides and hydroxysalts have been adapted and modified to prepare phase-pure materials. The beta-phases of nickel and cobalt hydroxide were characterised and shown to have highly crystalline brucite-type crystal structures of Ni(OH)₂ and Co(OH)₂ with no significant

amounts of anion incorporation. Alpha-phase nickel and cobalt hydroxides were successfully isolated and the compositions were determined to have a formula of M(OH)_{1.95}(H₂O)_{0.05}(NO₃)_{0.05} (where M = Ni, Co) which is consistent with the 'partial protonation' structure described by Kamath *et al.*¹⁹ for alpha-phase hydroxides. Layered hydroxynitrates that have formulae of M₃(OH)₄(NO₃)₂ (where M = Ni, Co) were also prepared and characterisation indicates they are isostructural to the previously reported Zn₃(OH)₄(NO₃)₂⁵³ and Mg₃(OH)₄(NO₃)₂⁵⁴ phases due to strong similarities in diffraction data, vibrational spectroscopy data and thermogravimetric data. The layered hydroxynitrate formula of M(OH)(NO₃)·H₂O (where M = Ni, Co and $x = 1.0$) were also prepared and are consistent with the phases prepared in the studies by Louër⁵⁵ and Petrov.⁵⁶ Solid-state and solution urea flux methods were determined to result in the formation and incorporation of cyanate anions in the parent hydroxide phases. The solid-state urea flux method formed mixed-anion layered hydroxysalt materials with $x = 0.67$, while solution methods formed alpha like phases consistent with the work of O'Hare. Additionally, powder X-ray diffraction analysis on its own was found to be insufficient for characterising layered hydroxide phases, particularly when the phases were poorly crystalline. Spectroscopic analysis must also be performed to enable characteristic bands of the incorporated anions to be used diagnostically to identify all phases present. These data are further complemented by the use of thermal methods to distinguish between different types of phase, since the broad continuous weight loss of alpha phases, contrasts markedly with the stepped losses of the hydroxysalts and the beta-phase. The ability to identify the different phases is particularly needed for the analysis of materials where hydroxides are used to make high purity industrial materials *e.g.* for electronics or catalysis.

Author contributions

Sam Wallbridge: methodology, investigation and writing – original draft. Kurt Lawson: methodology, investigation and writing – original draft. Amy Catling: methodology and investigation. Caroline Kirk: review and editing, supervision, project administration and funding acquisition. Sandra Dann: conceptualization, resources, writing – original draft, review and editing, supervision, project administration and funding acquisition.

Conflicts of interest

There are no conflicts to declare.

Acknowledgements

We thank the EPSRC/STFC for funding for KL and Loughborough University for the EPSRC/DTP Studentship for



SW. SCI are also thanked for their award of the Sydney Andrew Scholarship for SW. ICoNiChem are thanked for the donation of beta-cobalt hydroxide.

References

- H. Bode, K. Dehmelt and J. Witte, *Electrochim. Acta*, 1966, **11**, 1079–1087.
- J. McBreen, *Handbook of Battery Materials*, VCH, 1997.
- H. Cheng, A. D. Su, S. Li, S. T. Nguyen, L. Lu, C. Y. H. Lim and H. M. Duong, *Chem. Phys. Lett.*, 2014, **601**, 168–173.
- M. Aghazadeh, M. Ghaemi, B. Sabour and S. Dalvand, *J. Solid State Electrochem.*, 2014, **18**, 1569–1584.
- X. Yi, H. Sun, N. Robertson and C. Kirk, *Sustainable Energy Fuels*, 2021, **5**, 5236–5246.
- R. J. Mortimer, M. Z. Sialvi, T. S. Varley and G. D. Wilcox, *J. Solid State Electrochem.*, 2014, **18**, 3359–3367.
- M. Z. Sialvi, R. J. Mortimer, G. D. Wilcox, A. M. Teridi, T. S. Varley, K. G. U. Wijayantha and C. A. Kirk, *ACS Appl. Mater. Interfaces*, 2013, **5**, 5675–5682.
- Y. Chen, K. Rui, J. Zhu, S. X. Dou and W. Sun, *Chem. – Eur. J.*, 2019, **25**, 703–713.
- M. S. Vidhya, G. Ravi, R. Yuvakkumar, D. Velauthapillai, M. Thambidurai, C. Dang and B. Saravanakumar, *RSC Adv.*, 2020, **10**, 19410–19418.
- C. Y. Wang, S. Zhong, D. H. Bradhurst, H. K. Liu and S. X. Dou, *J. Alloys Compd.*, 2002, **330–332**, 802–805.
- R. D. Armstrong, G. W. D. Briggs and E. A. Charles, *J. Appl. Electrochem.*, 1988, **18**, 215–219.
- J. D. Donaldson and D. Beyersmann, *Ullmann's Encyclopedia of Industrial Chemistry*, 2005.
- R. S. McEwen, *J. Phys. Chem.*, 1971, **75**, 1782–1789.
- C. Greaves and M. A. Thomas, *Acta Crystallogr., Sect. B: Struct. Sci.*, 1986, **42**, 51–55.
- A. Arvinte, A. M. Sesay and V. Virtanen, *Talanta*, 2011, **84**, 180–186.
- D. Hunt, G. Garbarino, J. A. Rodríguez-Velamazán, V. Ferrari, M. Jobbagy and D. A. Scherlis, *Phys. Chem. Chem. Phys.*, 2016, **18**, 30407–30414.
- R. S. Jayashree and P. V. Kamath, *J. Mater. Chem.*, 1999, **9**, 961–963.
- P. V. Kamath, *J. Electrochem. Soc.*, 1994, **141**, 2956–2958.
- P. V. Kamath, G. H. Annal Therese and J. Gopalakrishnan, *J. Solid State Chem.*, 1997, **128**, 38–41.
- M. Mookherjee and L. Stixrude, *Am. Mineral.*, 2006, **91**, 127–134.
- P. Oliva, J. Leonardi, J. F. Laurent, C. Delmas, J. J. Braconnier, M. Figlarz, F. Fievet and A. de Guibert, *J. Power Sources*, 1982, **8**, 229–255.
- M. Sebastian, C. Nethravathi and M. Rajamathi, *Mater. Res. Bull.*, 2013, **48**, 2715–2719.
- Z. A. Hu, Y. L. Xie, Y. X. Wang, L. J. Xie, G. R. Fu, X. Q. Jin, Z. Y. Zhang, Y. Y. Yang and H. Y. Wu, *J. Phys. Chem. C*, 2009, **113**, 12502–12508.
- C. Faure, C. Delmas and M. Fouassier, *J. Power Sources*, 1991, **35**, 279–290.
- A. Delahaye-Vidal, B. Beaudoin, N. Sac-Epée, K. Tekaiia-Elhsissen, A. Audemer and M. Figlarz, *Solid State Ionics*, 1996, **84**, 239–248.
- M. Rajamathi, G. N. Subbanna and P. V. Kamath, *J. Mater. Chem.*, 1997, **7**, 2293–2296.
- Y. Du and D. O'Hare, *Inorg. Chem.*, 2008, **47**, 11839–11846.
- M. Rajamathi and P. V. Kamath, *Int. J. Inorg. Mater.*, 2001, **3**, 901–906.
- Y. Du and D. O'Hare, *Inorg. Chem.*, 2008, **47**, 3234–3242.
- Y. Du, K. M. Ok and D. O'Hare, *J. Mater. Chem.*, 2008, **18**, 4450–4459.
- D. S. Hall, D. J. Lockwood, C. Bock and B. R. MacDougall, *Proc. R. Soc. A*, 2015, **471**, 20140792.
- K. Petrov, N. Zotov, E. Mirtcheva, O. García-Martínez and R. M. Rojas, *J. Mater. Chem.*, 1994, **4**, 611–614.
- K. Petrov, A. Lyubchova and L. Markov, *Polyhedron*, 1989, **8**, 1061–1067.
- L. Markov, K. Petrov and V. Petkov, *Thermochim. Acta*, 1986, **106**, 283–292.
- M. Dixit, G. N. Subbanna and P. V. Kamath, *J. Mater. Chem.*, 1996, **6**, 1429–1432.
- T. N. Ramesh, *Inorg. Chem. Commun.*, 2011, **14**, 419–422.
- D. S. Hall, D. J. Lockwood, S. Poirier, C. Bock and B. R. MacDougall, *J. Phys. Chem. A*, 2012, **116**, 6771–6784.
- D. N. Sathyanarayana, *Vibrational Spectroscopy: Theory and Applications*, New Age International Limited, 2015.
- R. S. Jayashree and P. V. Kamath, *J. Power Sources*, 2001, **93**, 273–278.
- R. S. Jayashree and P. V. Kamath, *J. Appl. Electrochem.*, 1999, **29**, 449–454.
- T. Biswick, W. Jones, A. Pacuła and E. Serwicka, *J. Solid State Chem.*, 2006, **179**, 49–55.
- N. Thomas, *Mater. Res. Bull.*, 2012, **47**, 3568–3572.
- S. Angelov, M. Drillon, E. Zhecheva, R. Stoyanova, M. Belaiche, A. Derory and A. Herr, *Inorg. Chem.*, 1992, **31**, 1514–1517.
- Z. P. Xu and H. C. Zeng, *Chem. Mater.*, 1999, **11**, 67–74.
- M. Murthy, G. S. Nagarajan, J. W. Weidner and J. W. Van Zee, *J. Electrochem. Soc.*, 1996, **143**, 2319–2327.
- N. Iyi, F. Geng and T. Sasaki, *Chem. Lett.*, 2009, **38**, 808–809.
- R. W. Cairns and E. Ott, *J. Am. Chem. Soc.*, 1933, **55**, 527–533.
- M. C. Morris, H. F. Mcmurdie, E. H. Evans, B. Paretzkin, J. H. de Groot, B. S. Weeks and R. J. Newberry, *NBS Monograph 25*, 1978, p. 29.
- T. Sato, T. Nakamura and F. Ozawa, *J. Appl. Chem. Biotechnol.*, 1975, **25**, 583–590.
- I. F. Hazell and R. J. Irving, *J. Chem. Soc. A*, 1966, 669–673.
- P. Rabu, S. Angelov, P. Legoll, M. Belaiche and M. Drillon, *Inorg. Chem.*, 1993, **32**, 2463–2468.
- P. Gallezot and M. Prettre, *Bull. Soc. Chim.*, 1969, **2**, 407–409.



- 53 M. Louer, D. Grandjean and D. Weigel, *Acta Crystallogr., Sect. B: Struct. Crystallogr. Cryst. Chem.*, 1973, **29**, 1703–1706.
- 54 I. A. Kudrenko and Y. G. Dorokhov, *Russ. J. Inorg. Chem.*, 1973, **18**, 17.
- 55 M. Louër, D. Grandjean and D. Weigel, *Acta Crystallogr., Sect. B: Struct. Crystallogr. Cryst. Chem.*, 1973, **29**, 1703–1706.
- 56 K. Petrov, N. Zotov, O. Garcia-Martinez and R. Rojas, *J. Solid State Chem.*, 1992, **101**, 145–153.
- 57 L. Eriksson, D. Louër and P.-E. Werner, *J. Solid State Chem.*, 1989, **81**, 9–20.
- 58 K. N. Upadhyaya, *Analyst*, 1979, **104**, 375–377.
- 59 K. Nakamoto, *Handbook of Vibrational Spectroscopy*, American Cancer Society, 2006.
- 60 G. Adachi, N. Imanaka and Z. C. Kang, *Binary Rare Earth Oxides*, Springer, Netherlands, 2006.
- 61 V. R. Sastri, J. R. Perumareddi, V. R. Rao, G. V. S. Rayudu and J. C. G. Bünzli, *Modern Aspects of Rare Earths and their Complexes*, Elsevier Science, 2003.
- 62 J. W. Lee, J. M. Ko and J. D. Kim, *J. Phys. Chem. C*, 2011, **115**, 19445–19454.
- 63 C. Faure, C. Delmas and P. Willmann, *J. Power Sources*, 1991, **35**, 263–277.
- 64 T. N. Ramesh, *J. Solid State Chem.*, 2010, **183**, 1433–1436.
- 65 T. N. Ramesh, *Inorg. Chem. Commun.*, 2009, **12**, 832–834.

